Alexandria Engineering Journal (2022) 61, 305–314

HOSTED BY

Alexandria University

Alexandria Engineering Journal

www.elsevier.com/locate/aej
www.sciencedirect.com

Structure estimation of vertical axis wind turbine using artificial neural network

S. Teksin [a,c,*], N. Azginoglu [b], S.O. Akansu [a]

[a] Erciyes University, Faculty of Engineering, Department of Mechanical Engineering, Kayseri 38039, Turkey
[b] Kayseri University, Engineering Architecture and Design Faculty, Department of Computer Engineering, Kayseri 38280, Turkey
[c] Yuzuncu Yil University, Faculty of Engineering, Department of Mechanical Engineering, Van, 65080, Turkey

Received 26 October 2020; revised 26 April 2021; accepted 1 May 2021
Available online 08 June 2021

KEYWORDS

ANN;
Estimation;
Sustainable energy;
VAWT;
Wind;
Environment

Abstract Vertical axis wind turbines (VAWTS) can be a suitable choice for usage in urban areas. Wind conditions and structural parameters are critical to power production. In this study, some variations of a darrieus vawt was attempted via wind tunnel testing. A modified naca4412 blade profile was selected for this investigation. The influence of aspect ratios, angle of attack, chord length, etc. were investigated experimentally. After taken more than 800 data artificial neural network (ANN) was applied to estimate the other range of scales using different algorithms that are utilized the aforementioned experimental parameters. This study focuses on the design criteria and application of VAWTS inbuilt real environments without testing. The results have been promising and will provide ease of design for similar designs. Moreover, this work will contribute to environmental cleanup and a more livable world by increasing renewable energy resources.

© 2021 THE AUTHORS. Published by Elsevier BV on behalf of Faculty of Engineering, Alexandria University. This is an open access article under the CC BY-NC-ND license (http://creativecommons.org/licenses/by-nc-nd/4.0/).

1. Introduction

Wind is an atmospheric condition that moves from high pressure to low density by transferring kinetic energy of heat energy. Using this movement of the wind will contribute to the energy needs of the world. According to wind energy association, [1] wind energy capacity, together with other sustainable energy sources, was determined to be 95 tw. On the other hand, the combustion of fossil fuels emits massive quantities of greenhouse gas (ghg) into the atmosphere and endanger the future [2–4].

The air converted to kinetic energy can be generated by using wind turbines, which can be classified into two groups as horizontal axis wind turbine (hawts) and vertical axis wind turbine (vawts). This phenomenon has been made according to shaft architecture. If the wind is coming to the turbine shaft at an angle of 90 degrees, such turbines are called as vertical axis, while the wind flow and the rotor are parallel to each other, they are called as horizontal axis wind turbines. Hawts are used for most of the applications in flat areas in general. They also have big capacity generators that produce a tremendous amount of electrical power. These systems operate on-grid type, which means there is a connection between the wind power plant and the city power line. For rugged terrain such

* Corresponding author.
E-mail address: steksin@erciyes.edu.tr (S. Teksin).
Peer review under responsibility of Faculty of Engineering, Alexandria University.

https://doi.org/10.1016/j.aej.2021.05.002
1110-0168 © 2021 THE AUTHORS. Published by Elsevier BV on behalf of Faculty of Engineering, Alexandria University.
This is an open access article under the CC BY-NC-ND license (http://creativecommons.org/licenses/by-nc-nd/4.0/).

Nomenclature

a	area	t	torque
ann	artificial neural network	tu	turbulence intensity
c_p	power coefficient	v	wind speed
c	chord length	$u_\square$	free stream velocity
d	diameter of turbine	u_{rms}	root mean square velocity
d_p	plate diameter	a	angle of attack
d_h	shaft hole diameter	ρ	air density
h	height of airfoil	ω_r	angular velocity
p_t	turbine power	λ	tip speed ratio
p_w	wind power	σ	solidity
r	radius of turbine		

as settlements, towns, villages and city centers, usage of vawts are more suitable because of the kaleidoscopic wind direction and its speed [5]. The main advantage of these turbines is that they can take the wind from every direction. Also, they operate at low speed that technically is called tsr (tip speed ratio) caused low noise and less danger to flying animals. Carrigan *et al.* [6] have defined the essential parameters listed below;

$$\lambda = \frac{\omega_r R}{u_\infty} \tag{1}$$

$$C_p = \frac{P_T}{P_W} \tag{2}$$

$$P_W = \frac{\rho A V^3}{2} \tag{3}$$

$$P_T = \frac{2\pi n T}{60} \tag{4}$$

Where ω_r is the angular velocity, r is the radius of rotor, $u_\square$ is wind flow speed p_t is turbine power, p_w is wind power, ρ is air density, A is projection area of the turbine, V is wind speed, n is the rotation rate and T is the rotation torque. If it is desired that the power obtained is consistently at maximum, the rotor rotational speed must be adjusted according to the change of the wind speed so that the maximum power coefficient, c_p value can be obtained. In the case of advanced wind turbines, this arrangement is carried out automatically.

The problem is that turbines used, especially in urban areas with big crowds, also cause extra noise [7]. That's why the vertical axis wind turbine, which has small peripheral wind speed on the blades, is an excellent choice for low noise generation. Unfortunately, there are some disadvantages as well as the advantages of vertical axis turbines. For example, the self-starting capability of vawts is weak, which needs an initial movement on the blades.

Design parameters have essential effects on vawts. For example, blade configurations, types of blade, amount of attack angle, solidity are crucial criteria. More experimental and numerical studies are needed to overcome this complex problem. Moreover, as can be seen from the investigations, [8–11] cfd codes are used for special interests.

Investigation of the vertical axis wind turbine model in a wind tunnel showed that the number of blades affects the rotation of the rotor in a wind turbine. Increasing the number of turbine blades makes it easy for the wind turbine to operate at a low free stream. Sunyoto et al. [12] showed that the three-blade systems more reliable than two and four-blade configurations. The aspect ratio of a turbine is another crucial parameter for performance characteristics as well as system affects the coefficient of power, c_p. Brusca *et al.* [13] showed an increase in the aspect ratio causes a decrease in the power coefficient. Moreover, d'ambrosio and medaglia [14] determined that vawts have two peak points of their torques both in front and rear of the turbine as a sinusoidal graph.

There are some studies to predict wind power generation and, mainly, the estimation of the turbine's structure minimizes the effort and investment cost spent on the production stage. For this reason, within the scope of this study, firstly, studies using the intelligent algorithm and smart systems in the literature have been examined.

Intelligent algorithms have been used in almost all branches of engineering, especially in recent years [15,16]. This situation has provided many benefits such as lowering design costs, reducing energy consumption and increasing efficiency, designing in ideal time, minimizing costs, and maximizing performances. When the studies in the literature are examined, it is seen that there are studies involving optimization [17,18] and, more specifically, soft computing [15], Fuzzy logic based [17], and Adaptive neuro-fuzzy inference system (ANFIS) [19–21]. Besides, there are also Support Vector Machine (SVM) studies in the field of Artificial Intelligence (AI) and, in particular, machine learning [22,23]. Among these studies, analysis [24–26] and forecasting [25,27–31] have an important place. Another study used ANN for estimation [32].

Intelligent algorithms and systems are used extensively in energy studies as well as in many areas. Petkovic et al. [33] used ANN to predict wind speed, while Nikolic et al. made use of neuro-fuzzy systems [34]. Petkovic et al. Used neuro-fuzzy strategies to make wind farms more efficient. There are also neuro-fuzzy, and ANFIS studies conducted to make wind turbines more efficient and less costly [35–38].

ANN is another field of application for wind turbines. The application area of the artificial intelligence algorithms that are known is very extensive. A reasonable work was applied to wind farms using ann by Mabel and Fernandez [39]. They collected data for three years and developed a model in matlab software. While wind speed, relative humidity and generation hours are input data, power production is output. Also, the number of the hidden layers are 5. In other words, 3–5-1 archi-

tecture was employed for optimum solution. They found that an artificial neural network can be used as an efficient mechanism to guess energy production from wind farms.

According to another predictive study Cam *et al.* [40], average wind speed and wind power were estimated with the aid of ann in whole regions of turkey. moreover, they determined the proper wind farms selection and used a smaller number of stations to collect data. Categorization was made for seven different geographic areas of turkey, and they depicted that mean error levels were within the acceptable range.

Within the scope of this study, firstly, the parameters affecting the voltage and current production of naca4412 profile three-bladed vertical axis wind turbine (vawt) were analyzed by changing the chord length, aspect ratios, angle of attack and wind flow regime, etc. After the data collection phase structure estimation was employed by using artificial neural network. Both estimation work has been carried out, and the strategies to be used in data separation have also been analyzed. Besides, the performances of three different ANN-based algorithms were compared, and it was determined which algorithm should be selected for different data amounts. Also, the effect of the number of hidden units on the performance was measured. Algorithms have been evaluated in terms of both time cost and success rate.

High success rates have been achieved in the experiments. As the numerical studies guide us before spending a lot of money and investing, the neural network generated within the scope of this study will prevent wasting time and shed light on us for a broader range of applications.

2. Materials and methods

In this section, the steps of the prediction process are mentioned first. next, the dataset used to measure the success of the experiments is explained. Then, the description of the artificial neural network to be used is given. finally, the results obtained by experimenting with different learning algorithms and parameters are presented.

2.1. Estimation process steps

The general process steps are given in (Fig. 1). Firstly, a preliminary study was conducted, and an experimental setup was established to collect data. The parameters such as blade profile, chord lengths, angle of attack, turbine diameter, blade length, frequency of fan, wind speed, current, resistance, speed, voltage used during the experiment were changed. The obtained data set was subjected to data cleaning, integration, and reduction to achieve higher estimation results. Then, this data set was used in the artificial neural network, which was generated, and related results were produced. Finally, the findings were evaluated.

2.2. Experimental set-up of wind turbine

Experiments were employed in an open-loop wind tunnel that is shown in (Fig. 2). This suction type tunnel was controlled with 1 m diameter 15 kw electrical motor. The testing section has 1800 mm length and entrance of the test section 570 × 570 mm dimensions. To keep constant the static pressure of the flow, the outlet has a 590 × 590 mm cross-

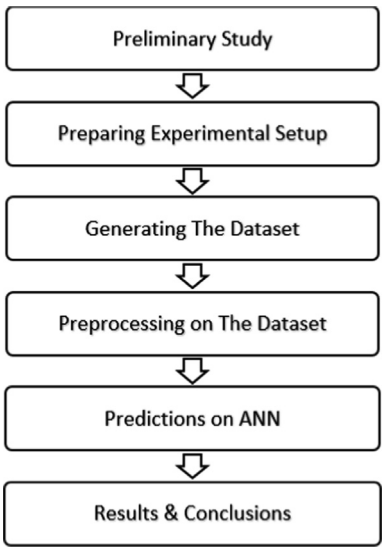


Fig. 1 estimation process step chart.

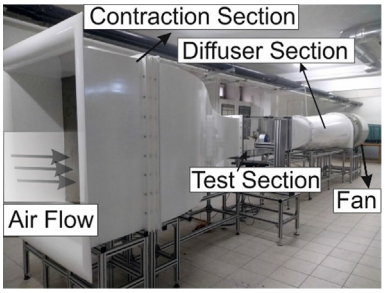


Fig. 2 wind tunnel testing set-up.

sectional area with an increasing 3^0 angles. The operational speed range is between 3 and 33 m/s and also the maximum speed achieved when the test section is empty. According to the study of yilmaz et al. [41] turbulence intensity *tu*, which is a dimensionless parameter, was measured less than 1% by using dantec dynamics pro streamline hot-wire anemometer, cta (constant temperature anemometer) system. This phenomenon has provided more accurate and reliable results in the research. The equations used in the measurement system are listed below:

$$Tu(\%) = \frac{u_{rms}}{\bar{U}} \times 100 \tag{5}$$

$$u_{rms} = \sqrt{\sum_{i=1}^{n} \frac{(U_i - \bar{U})^2}{n-1}} \tag{6}$$

Where $\bar{U}$ is the time-averaged value of the streamwise velocity, u_{rms} is the root mean square of velocity fluctuations in the streamwise direction.

A schematic representation of the wind tunnel, including to wind turbine, is shown in (Fig. 3). The turbine shaft and generator are connected with coupling by reaming on the lathe, the one side 10 mm and the other side 4 mm. The coupling has a small space that minimizes the vibration during the rotation along the x-axis.

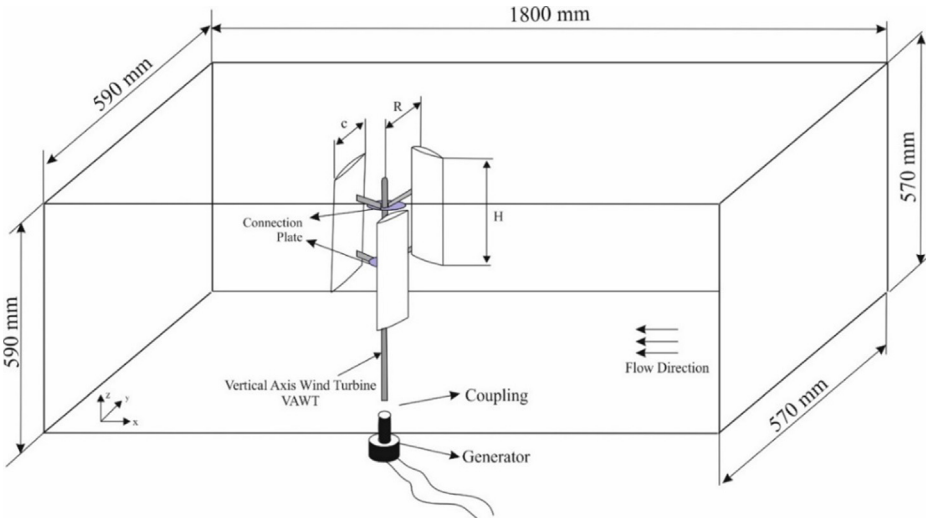


Fig. 3 schematic representation of the experimental setup.

Three-bladed vertical axis wind turbine, vawt with asymmetric airfoil naca4412 profile, was used. The blades are designed in a commonly used cad program and produced in a 3d printer by obtaining g-codes with the slicing software. even though it is tried to create a sensitive and suitable environment during the production of the blades, some roughness occurs on them. Sanding is applied for both sides in 4 steps to minimize this problem. by making changes on this blade profile, cavities were formed on the blade to generate more force by taking more wind. (Fig. 4) demonstrates the general seeming of the blade with cavities at a and airfoil coordinate in the 2d sketch at b. moreover, data information such as the camber and thickness of the naca4412 blade profile is given in (Table 1).

In experiments, blades chord length, turbine diameter, angle of attack was changed for under several wind flow regimes. Three different blades chord lengths are 40, 60 and, 80 mm at 300 mm heights were used. each blade was connected to the central shaft with aluminum bars having the 3 mm $\times$ 20 mm diameters. The turbine diameter also changed by altering the bar length and, the blades are fixed to the turbine shaft at two different points. The main problem is that the angle of attack can be adjusted correctly. An aluminum connection plate is designed, as shown in (Fig. 5), for accurate measurements. Although it is difficult to machine aluminum material, it has been preferred in this system due to its lightweight. This body has 100 mm diameters and a 10 mm hole for the shaft location. Instead of the aluminum shaft, the carbon rod was selected to eliminate permanent deformation on it during rotation, especially at a high revolution. Five same holes drilled both on the plate and connection bars in laser cut. The holes, which are named with the letters, are screwed with the holes in the bars at two different points. Each hole corresponds to 5 degrees in between, while one is always constant at point a. In other words, if a-b is fixed, it means the zero angles of attack was formed. When the a-c or a-d is fixed, 5^0, 10^0 attack angles achieved, respectively. The fastening of

Table 1 blade (naca4412) data information.

max camber (%)	4
max camber position (%)	40
thickness (%)	12

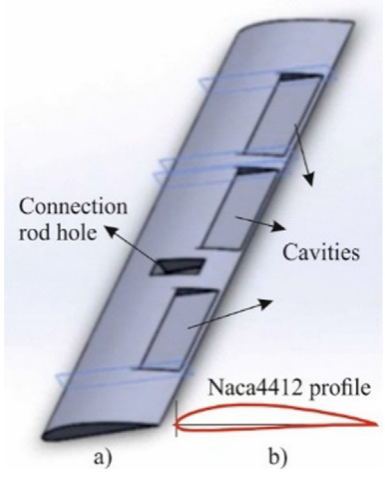


Fig. 4 naca4412 blade (a) and schematic representation (b).

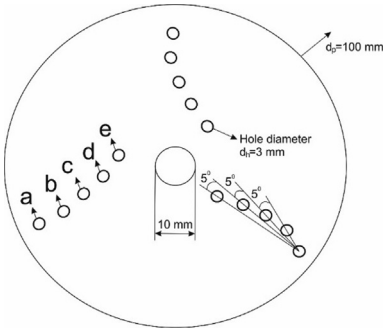


Fig. 5 details of connection plate.

the connection plate with rod is tightened with a fiber nut for both safeties and to prevent separation at rotational speeds above 1000 rpm.

The rotor diameters of the vawt 200, 300 and, 400 mm, which corresponds to the aspect ratio is 0,66, 1 and, 1,33, respectively. These values are appropriate in the range of $0{,}5 < ar_{opt}$ less than 2 in investigation of ahmadi and carriveau, [42] for vertical axis wind turbine. furthermore, another important parameter is solidity, which affects the performance characteristics of vawts. The solidity ratio, σ, declares the relations between the total blade area and turbine projection area which is defined as;

$$\sigma = \frac{A_b}{A_S} = \frac{Nc}{D} \tag{7}$$

Where n is the number of the blade, c is chord length and d is the turbine diameter. It changes between 0,3 and 1,2 where classified under optimum range and high-solidity frame [43]. Detail values are given in table 2 according to cord length and turbine diameters.

After adjusting the frequency value of electrical motor, wind velocities were measured using a pitot tube through the small hole in the test area of the wind tunnel. This process should be repeated before starting each experiment because, shape and size of the body which is located in the test section can be affect the free stream flow velocity. To observe at which wind speed the turbine self-starts it was measured at zero load first, causing only voltage values. After that, 100 O, 500 O, 1 k ohms and 0 k ohms resistors were connected serially to load the system and power was obtained. voltage and current values were taken concerning connected resistors.

2.3. Dataset

The dataset produced by wind tunnel testing set-up is primarily pre-processed. As a result of the pre-processing, some rows and columns were pruned from the dataset to be used to improve the performance of the Ann architecture. The angle of attack, turbine diameter, wind speed, chord length, and resistance columns were determined to be presented as input to the ann. The output of the network is the voltage column. In other words, the amount of electricity produced according to the state of the other parameters will be estimated. Dataset is divided into three parts as training, validation and testing. A few sample data are given in table 3.

2.4. Methodology of ann model

A Shallow (a standard two-layer) ann architecture is preferred because the dataset to be used in the estimation does not have very dense content. This network has five inputs (angle of attack, turbine diameter, wind speed, chord length and, resistance) and one output (the voltage). In the experiments, different numbers of hidden neurons were used in the hidden layer. (Fig. 6) shows an ann architecture with five inputs, one output, and ten hidden neurons (the figure generated from http://alexlenail.me/nn-svg).

The sigmoid transfer function was used in the hidden layer and the linear transfer function was used in the output layer. levenberg–marquardt, more, [43] bayesian regularization, Williams [44] and scaled conjugate gradient, moller [45] algorithms were used as learning algorithms. A summary of these algorithms is given below.

- Levenberg-marquardt algorithm: there is an inversely proportional relationship between memory usage and speed in algorithms. In general, this algorithm uses more memory, but it works fast. With these features, it is an ideal algorithm for small and medium-size problems [46].
- Scaled conjugate gradient algorithm: needs less memory than the other algorithms. It also uses less time, but the success rate is lower than the others, moller [45].
- Bayesian regularization algorithm: the slowest algorithm compared to others. It takes more time but is more successful especially in small and noisy data sets, williams [44].

Before network training, the data were normalized according to the mapminmax method. In this way, the bias of the system according to significant valued parameters (such as resistance or turbine diameter) is prevented. Wang and bovik, [4] presented two different evaluation criteria, mean squared error (mse) and regression (r) were used to measure the predictive success. The mse is the square of the average error between the estimated value and the actual value. A low mse value means good performance, and a value of 0 corresponds to

Table 2 aspect ratios and solidity values for each turbine structure.

turbine diameter, d	200 mm			300 mm			400 mm		
chord length, c	40 mm	60 mm	80 mm	40 mm	60 mm	80 mm	40 mm	60 mm	80 mm
solidity, σ	0.6	0.9	1.2	0.4	0.6	0.8	0.3	0.45	0.6

Table 3 a bunch of sample data from the dataset.

input	data index	40	220	407	513
	chord length	40	60	80	80
	angle of attacks	10	5	5	15
	turbine diameter	200	200	200	300
	wind speed	5,05	7,01	5,05	9,08
	resistance	1000	1000	500	10,000
output	voltage	0,465	5,86	3,5	5,45

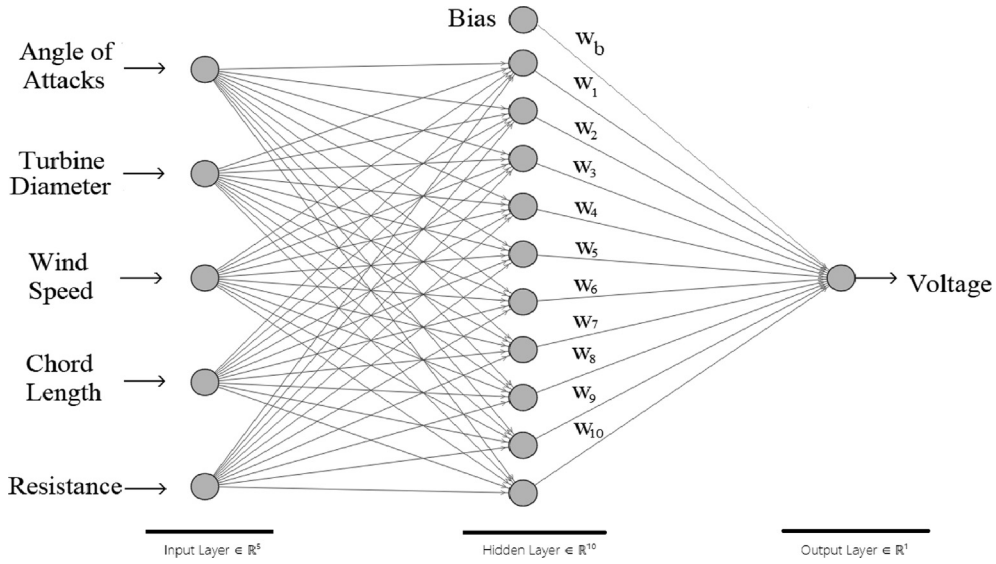


Fig. 6 the architecture of the ann.

the actual value. Regression refers to the correlation between the estimated value and the actual value.

3. Results and discussion

3.1. Dataset partitioning experiment

In this experiment, how the dataset should be partitioned was examined. When we look at the literature, in the study conducted by Genc and Tunc [47]. It was stated that the most common choice is 70/15/15. In the study of alqahtani et al., the 80/10/10 method was taken as a basis alqahtani and whyte 2016 [48]. Andrew, [49] ng prefers 60/20/20 or 70/30, and if the data is big 98/1/1 in his coursera course. In the article by Rachel draelos, [50] it is noted that frequent uses are generally 70/15/15, 60/20/20, and 80/10/10, and the best choice should be found by experimenting. for this purpose, the data set was subjected to 5 different parts. These are 50/25/25, 60/20/20, 70/15/15, 80/10/10, 90/5/5, and 98/1/1. In general, 98/1/1 is recommended when the number of data amount reaches millions. If the number of data is expressed in thousands, the most common use is 70/15/15. However, there is no objective selection method on how to do this partition because each data has its own unique features. The most logical way is to test which partitioning performs better. This experiment is intended to guide people with similar data.

In the experiments, most of the data was reserved for training, and the remainder was split into two equal parts as validation and testing. for example, in the 50/25/25 experiment, the data was split into 50% training, 25% validation, and 25% test data. The test results obtained are given in table 4.

According to these results, increasing the education data has a good reflection on the results in general. This situation shows that our data has its characteristics. The fact that the training data has increased too much has decreased the success rate. According to the results in the table, it is seen that the ideal results for our data are obtained in 90/5/5 partitioning. It is clear that different partitioning gives good results according to different data amounts and characteristic features of different data. In this case, it is clear that better results will be obtained in testing the segmentation by experimenting.

3.2. Learning algorithm experiment

In this experiment, learning algorithms were tested. The number of hidden neurons is set to 10. each learning algorithm was tested 50 times and the results of these 50 experiments were averaged. The results are given in table 5 and table 6.

According to the results, bayesian regularization algorithm showed the best performance. It was followed by levenberg–marquardt and scaled conjugate gradient algorithms, respectively. The working times (runtime) of the algorithms are given in table 7.

Table 4 regression results of the dataset partioning experiments.

partioning	all r	test r	train r	val r
50/25/25	0.9777	0.9639	0.9913	0.9649
60/20/20	0.9837	0.9696	0.9927	0.9703
70/15/15	0.9879	0.9741	0.9929	0.9785
80/10/10	0.9911	0.9784	0.9937	0.9832
90/5/5	0.9928	0.9831	0.9937	0.9856
98/1/1	0.9859	0.9760	0.9859	0.9850

Table 5 regression results of the learning algorithms experiments.

regression results (0–1)				
	training	validation	test	all
levenberg–marquardt	0.9839	0.9772	0.9766	0.9818
bayesian regularization	0.9870	nan*	0.9796	0.9859
scaled conjugate gradient	0.9423	0.9416	0.9328	0.9408

*the bayesian regularization algorithm does not require validation.

Table 6 performance results of the learning algorithm experiments.

performance results (mse)				
	training	validation	test	all
levenberg–marquardt	0.1475	0.2085	0.2169	0.1670
bayesian regularization	0.1119	nan	0.1835	0.1294
scaled conjugate gradient	0.5163	0.5368	0.6001	0.5318

Table 7 runtimes of the algorithms.

runtimes of the algorithms (seconds)	
levenberg–marquardt	43.11
bayesian regularization	129.28
scaled conjugate gradient	33.99

The algorithm with the longest runtime is bayesian regularization. The following inference can be made according to the table 5; if the dataset is significant, the levenberg–marquardt algorithm may be preferred to avoid the cost of calculation. The bayesian-regularization algorithm should be selected if the dataset is not too big or if the calculation time is not very important and the accuracy is essential.

The bayesian regularization algorithm is more suitable for our problem since the data density is not very high, and accuracy is more critical for us.

3.3. Hidden neuron experiment

In the next experiment, we examined how the number of hidden neurons affects educational performance. The bayesian regularization algorithm is chosen for the training algorithm because it gave the best results in the previous experiment. experiments were performed by increasing the number of hidden neurons between 5 and 50. These experiments were repeated 50 times to ensure consistent results, and the results were averaged. The results obtained are given in the tables below. regression (r) results are given in the table 8 and fig. 7; error rate (mse) is given in the table 9 and fig. 8 and algorithm run times are given in the table 10 and fig. 9.

The algorithm runtime (seconds) is determined by dividing the experiment time to 50 to find the approximate completion time of each experiment.

When the results are evaluated, it is seen that the best performance is obtained with 35 hidden neurons. Furthermore,

Table 8 hidden unit experiment regression results.

hidden unit experiment regression results			
training	test	all	hidden units
0,9755	0,9694	0,9746	5
0,987	0,9796	0,9859	10
0,9944	0,9897	0,9937	15
0,9974	0,9933	0,9968	20
0,9987	0,9947	0,9981	25
0,9992	0,996	0,9987	30
0,9994	0,9962	0,9989	35
0,9996	0,9945	0,9988	40
0,9993	0,9933	0,9984	45
0,9997	0,9927	0,9986	50

when the algorithm runtimes are considered, it is seen that the runtime increases approximately logarithmically. In this case, the selection of more than 35 hidden neurons will cause a decrease in performance, as well as a reasonable period of study time seems to be over. If the number of hidden neurons is less than 35, the success rate and working time are decreased. Under these conditions, it would be reasonable to select the number of hidden neurons as 35.

3.4. Experiment with the ideal parameters

Ideal training algorithm and number of hidden layers have been determined with previous experiments. The following results (table 11) were obtained by using the determined number of the hidden layer (35) and the training algorithm (the bayesian regularization).

4. Summary and Conclusıon

In this study, vertical axis wind turbine, vawt, was investigated in a wind tunnel system. This type of turbine has been affected

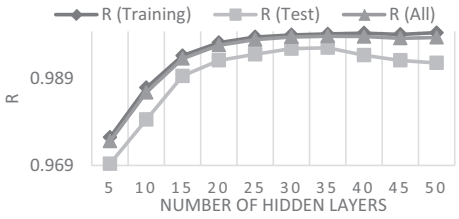


Fig. 7 graphic of hidden unit experiment regression results.

Table 9 hidden unit experiment performance (mse) results.

hidden unit experiment performance (mse) results			
training	test	all	hidden units
0,2242	0,2737	0,2316	5
0,1119	0,1835	0,1294	10
0,0515	0,0957	0,0581	15
0,0237	0,0648	0,0298	20
0,0122	0,0488	0,0177	25
0,0076	0,0367	0,0019	30
0,0052	0,0367	0,0099	35
0,0037	0,0525	0,011	40
0,0062	0,0623	0,0146	45
0,0028	0,0685	0,0126	50

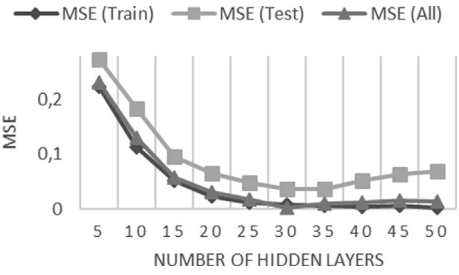


Fig. 8 graphic of hidden unit experiment performance (mse) results.

Table 10 hidden unit experiment algorithm runtime comparison.

hidden unit experiment algorithm runtime comparison		
runtime (sec)	average runtime (runtime / 50) (sec)	hidden units
63,79	1,2758	5
129,28	2,5856	10
240,07	4,8014	15
560,38	11,2076	20
607,5	12,15	25
1423,86	28,4772	30
2610,31	52,2062	35
4410,71	88,2142	40
5091,45	101,829	45
7126,74	142,5348	50

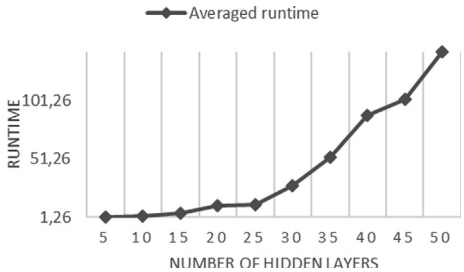


Fig. 9 graphic of hidden unit experiment algorithm runtime comparison.

Table 11 results of ideal parameters experiment.

bayesian regularization with 35 neurons	
evaluation criteria	results
regression (test)	0.9997
regression (train)	0.9905
regression (all)	0.9983
performance (mse)	0.0161
train performance (mse)	0.0031
time	277,59 sec

by lots of parameters such as chord length, aspect ratios, angle of attack etc. The results obtained by changing these data are listed below:

- Modified naca4412 airfoil profile was used for this experiment in open circuit wind tunnel set-up.
- Blade produced in 3d printer from polymeric material pla and smoothed to eliminate/minimize the roughness on the surface using sand paper at 4 stages.
- In order to observe at which wind speed the turbine self-starts it was measured at zero load first. After that, resistors ranging from 100 to 10 k ohms resistors were connected serially to load the system and power was obtained. Voltage and current values were taken with respect connected resistors.
- Wind speed was altered from 3 m/s to 9 m/s by changing the frequency controller of the fan. At each steps wind speed was measured using a pitot tube in the test area.
- structure parameters of the turbine were changed as chord length, turbine diameter, angle of attack, wind speed. In the experiments, more than 800 data were obtained.
- The data obtained were used in an artificial neural network training to be used in energy production estimation
- An ann architectural solution to similar problems has been identified.

Consequently, the architecture which we have generated for estimation can be used as ready (the problem does not have to be exactly the same) in a system with a similar data type. This learnt artificial neural network can be used in order to make best use of its efficient designs of these types of vertical axis wind turbines in rural area. The results obtained showed that this network we trained can be guide and used in the design of similar systems.

Future works

- The ann architecture we generated will be installed on a server. Thus, direct estimations can be made in the ready-trained system for similar problems. public access will be available also.
- Different training algorithms are planned to be implemented.
- It is planned to increase the number of data and use deep learning techniques.

Declaration of Competing Interest

The authors declare that they have no known competing financial interests or personal relationships that could have appeared to influence the work reported in this paper.

Acknowledgements

This work was supported in part by the Scientific And Technological Research Council Of Turkey, Tubıtak under grant no. 315M478 and the doctorate foundation of Erciyes University, Scientific Research Center, Project No: 9685.

References

[1] Wind Energy 2050. A wwea technical committee report on grid integration. World Wind Energy Association; 2015.
[2] Q.S. Li, Z.R. Shu, F.B. Chen, Performance assessment of tall building-integrated wind turbines for power generation, Appl. Energy. 165 (2016) 777–788.
[3] Z. Cheng, M. Ha, Z. Gao, T. Moan, Effect of the number of blades on the dynamics of floating straight-bladed vertical axis wind turbines. *Renew*, Energy 101 (2017) 1285–1298.
[4] Z. Wang, A.C. Bovik, Mean squared error: love it or leave it? a new look at signal fidelity measures, Ieee Signal Processing Magazine 26 (1) (2009) 98–117.
[5] H.Y. Peng, H.F. Lam, Turbulence effects on the wake characteristics and aerodynamic performance of a straight-bladed vawt by wind tunnel tests and large eddy simulations, Energy. 109 (2016) 557–568.
[6] T.J. Carrigan, B.H. Dennisi, Z.X. Han, B.P. Wang, Aerodynamic shape optimization of a vertical-axis wind turbine using differential evolution, isrn *Renew*, Energy (2012) 1–16.
[7] F. Balduzzi, A. Bianchini, E.A. Carnevale, L. Ferrari, S. Magnani, Feasibility analysis of a darrieus vertical-axis wind turbine installation in the rooftop of a building, Appl Energy 97 (2012) 921–929.
[8] M. Abkar, J.O. Dabiri, Self-similarity and ow characteristics of vertical-axis wind turbine wakes: an les study, J. Turbul. 18 (2017) 373–389.
[9] F. Trivellato, M. Raciti Castelli, on the courant-friedrichs-lewy criterion of rotating grids in 2d vertical-axis wind turbine analysis, *Renew*, Energy 62 (2014) 53–62.
[10] S. Shamsoddin, F. Porte-Agel, large eddy simulation of vertical axis wind turbine wakes, Energies 7 (2014) 890–912.
[11] Bottasso, C., Campagnolo, F., Petrovic, V. Wind tunnel testing of scaled wind turbine models: beyond aerodynamics, J. Wind Eng. İnd. Aerod. 2014; 127 11-28.
[12] Sunyoto, A., Wenehenubun, F., And Sutanto, H., (2013). the effect of number of blades on the performance of h-darrieus type wind turbine. in qir (quality in research), İnternational Conference On. 2013. ieee.
[13] S. Brusca, R. Lanzafame, M. Messina, Design of a vertical-axis wind turbine: how the aspect ratio affects the turbine's performance, Int J Energy Environ Eng 5 (4) (2014) 333–340.
[14] D'ambrosio, M. And Medaglia, M. Vertical axis wind turbines: History, Technology And Applications 2010.
[15] J. Katebi, M. Shoaei-parchin, M. Shariati, N.T. Trung, M. Khorami, Developed comparative analysis of metaheuristic optimization algorithms for optimal active control of structures, Engineering with Computers (2019) 1–20.
[16] M. Fayed, M. Elhadary, H. Ait Abderrahmane, Bassem Nashaat Zakher, Yarn Tensile Properties Modeling Using Artificial Intelligence, Alexandr. Eng. J. 59 (2020) 4435–4440.
[17] A. Ziaei-Nia, M. Shariati, E. Salehabadi, Dynamic mix design optimization of high-performance concrete, Steel and Composite Structures 29 (1) (2018) 67–75.
[18] A. Toghroli, M. Suhatril, Z. Ibrahim, M. Safa, M. Shariati, S. Shamshirband, Potential of soft computing approach for evaluating the factors affecting the capacity of steel-concrete composite beam, Journal of Intelligent Manufacturing 29 (8) (2018) 1793–1801.
[19] M. Mohammadhassani, H. Nezamabadi-Pour, M. Suhatril, M. Shariati, An evolutionary fuzzy modelling approach and comparison of different methods for shear strength prediction of high-strength concrete beams without stirrups, Smart Struct Syst Int J 14 (5) (2014) 785–809.
[20] Y. Sedghi, Y. Zandi, M. Shariati, E. Ahmadi, V. Moghimi Azar, A. Toghroli, M. Safa, E. Tonnizam Mohamad, M. Khorami, K. Wakil, Application of ANFIS technique on performance of C and L shaped angle shear connectors, Smart Structures and Systems 22 (3) (2018) 335–340.
[21] I. Mansouri, M. Shariati, M. Safa, Z. Ibrahim, M. Tahir, D. Petković, Analysis of influential factors for predicting the shear strength of a V-shaped angle shear connector in composite beams using an adaptive neuro-fuzzy technique, Journal of Intelligent Manufacturing 1–11 (2017).
[22] M. Safa, M. Shariati, Z. Ibrahim, A. Toghroli, S.B. Baharom, N.M. Nor, D. Petkovic, Potential of adaptive neuro fuzzy inference system for evaluating the factors affecting steel-concrete composite beam's shear strength, Steel and Composite Structures 21 (3) (2016) 679–688.
[23] E. Sadeghipour Chahnasir, Y. Zandi, M. Shariati, E. Dehghani, A. Toghroli, E.T. Mohamed, A. Shariati, M. Safa, K. Wakil, M. Khorami, Application of support vector machine with firefly algorithm for investigation of the factors affecting the shear strength of angle shear connectors, Smart structures and systems 22 (4) (2018) 413–424.
[24] Srđjan J., Amir S. D., Emran Y., Obrad A., Dalibor P. and Shahaboddin S., Forecasting of Underactuated Robotic Finger Contact Forces by Support Vector Regression Methodology, International Journal of Pattern Recognition and Artificial Intelligence, DOI: 10.1142/S0218001416590199, Volume 30, Issue 07, 2016, pp. 1-11
[25] A. Shariati, T. Schumacher, N. Ramanna, Eulerian-based virtual visual sensors to detect natural frequencies of structures, Journal of Civil Structural Health Monitoring 5 (4) (2015) 457–468.
[26] Dalibor P., Srdjan J., Obrad A., Bogdan N., Branko P., Analyzing of flexible gripper by computational intelligence approach, Mechatronics, DOI: 10.1016/j.mechatronics.2016.09.001, Volume 40, December 2016, pp. 1-16.
[27] N.T. Trung, A.F. Shahgoli, Y. Zandi, M. Shariati, K. Wakil, M. Safa, M. Khorami, Moment-rotation prediction of precast beam-to-column connections using extreme learning machine, STRUCTURAL ENGINEERING AND MECHANICS 70 (5) (2019) 639–647.
[28] M. Shariati, N.T. Trung, K. Wakil, P. Mehrabi, M. Safa, M. Khorami, Moment-rotation estimation of steel rack connection

using extreme learning machine, Steel And Composıte Structures 31 (5) (2019) 427–435.
[29] Na.da. Osman, Marwan Torki, Mustafa ElNainay, Abdulrahman AlHaidari, Emad Nabil, Artificial Intelligence-Based Model for Predicting the Effect of Governments' Measures on Community Mobility, Alexandr. Eng. J. 60 (2021) 3679–3692.
[30] M. Fayed, M. Elhadary, H. Ait Abderrahmane, Bassem Nashaat Zakher, The ability of forecasting flapping frequency of flexible filament by artificial neural network, Alexandr. Eng. J. 58 (2019) 1367–1374.
[31] A. Toghroli, M. Mohammadhassani, M. Suhatril, M. Shariati, Z. Ibrahim, Prediction of shear capacity of channel shear connectors using the ANFIS model, Steel Compos Struct 17 (5) (2014) 623–639.
[32] M. Mohammadhassani, H. Nezamabadi-Pour, M. Suhatril, M. Shariati, Identification of a suitable ANN architecture in predicting strain in tie section of concrete deep beams, Struct. Eng. Mech 46 (6) (2013) 853–868.
[33] D. Petković, V. Nikolić, V.V. Mitić, L. Kocić, Estimation of fractal representation of wind speed fluctuation by artificial neural network with different training algorothms, Flow Measurement and Instrumentation 54 (2017) 172–176.
[34] V. Nikolić, V.V. Mitić, L. Kocić, D. Petković, Wind speed parameters sensitivity analysis based on fractals and neuro-fuzzy selection technique, Knowledge and Information Systems 52 (1) (2017) 255–265.
[35] D. Petković, N.T. Pavlović, Ž. Ćojbašić, Wind farm efficiency by adaptive neuro-fuzzy strategy, International Journal of Electrical Power & Energy Systems 81 (2016) 215–221.
[36] B.A. Aamer, L. Xiaodong, Adaptive neuro-fuzzy approach for wind turbine power coefficient estimation, Renewable and Sustainable Energy Reviews 28 (December 2013) 191–195.
[37] P. Dalibor, Ć. Žarko, N. Vlastimir, S. Shahaboddin, L. Miss, K. Mat, B.A. Nor, W.A.W. Ainuddin, Adaptive neuro-fuzzy maximal power extraction of wind turbine with continuously variable transmission, Energy 64 (January 2014) 868–874.
[38] Dalibor P., Siti A. H., Žarko Ć., Nenad P., Adapting project management method and ANFIS strategy for variables selection and analyzing wind turbine wake effect, Natural Hazards, DOI: 10.1007/s11069-014-1189-1, Volume 74, Issue 2, November 2014, pp. 463-475.
[39] Mabel, M. C., And Fernandez, E. Estimation of energy yield from wind farms using artificial neural networks. ieee transactions on energy conversion 2009; 24(2), 459-464.
[40] E. Cam, E. Arcaklioglu, A. Cavusoglu, B. Akbiyik, A classification mechanism for determining average wind speed and power in several regions of turkey using artificial neural networks, Renewable Energy 30 (2) (2005) 227–239.
[41] İ. Yilmaz, S. Keiyinci, O. Cam, A. Karci, Çırpan kanadın aerodinamik parametrelerinin deneysel olarak incelenmesi, Journal Of The Faculty Of Engineering And Architecture of Gazi University 32 (4) (2017) 1035–1050.
[42] M. Ahmadi-Baloutaki, R. Carriveau, Ting Ds-K, Straight-bladed vertical axis wind turbine rotor design guide based on aerodynamic performance and loading analysis, P*roc Inst Mech Eng, Part A: j power energy* 228 (2014) 718–741.
[43] J.J. Moré, The levenberg-marquardt algorithm: *Implementation and theory in numerical analysis*, Springer, Berlin, heidelberg, 1978, pp. 105–116.
[44] P.M. Williams, bayesian regularization and pruning using a laplace prior, Neural Computation 7 (1) (1995) 117–143.
[45] M.F. Møller, A scaled conjugate gradient algorithm for fast supervised learning, neural networks 6 (4) (1993) 525–533.
[46] H. Yu, B. Wilamowski, M. Levenberg-marquardt training. *İndustrial Electronics Handbook* 5 (12) (2011) 1.
[47] B. Genc, H. Tunç, Optimal training and test sets design for machine learning, Turkish Journal Of Electrical Engineering & Computer Sciences 27 (2) (2019) 1534–1545.
[48] A. Alqahtani, A. Whyte, Estimation of life-cycle costs of buildings: regression vs artificial neural network, Built Environment Project And Asset Management (2016).
[49] Andrew N.G. https://www.coursera.org/lecture/deep-neural-network/train-dev-test-sets-cxg1s (2017, accessed 1 february 2020)
[50] Draelos R. https://glassboxmedicine.com/2019/09/15/best-use-of-train-val-test-splits-with-tips-for-medical-data/ (2019, accessed 1 february 2020).